29th International Cosmic Ray Conference Pune (2005) **00**, 101–106

Air Shower Properties with the Gluon Saturation Model BBL

H.J. Drescher

Frankfurt Institute for Advanced Studies (FIAS), Johann Wolfgang Goethe-Universität, Max-von-Laue-Straße 1, 60438 Frankfurt am Main

Presenter: H.J. Drescher (h.j.drescher@fias.uni-frankfurt.de), HE.1.4

The hadronic interaction model BBL implements the ideas of gluon saturation due to large densities. When approaching the black body limit at high energies, leading partons acquire large transverse momenta which breaks up their coherence. This leads to a suppression of forward scattering, and is therefore important for air showers. We discuss some general aspects of this new approach and their influence on air shower properties as seen by fluorescence and surface detectors: The position of the shower maximum is reduced due to stronger absorption in the atmosphere. The lateral distribution functions become flatter for the same reason. Muons are produced abundantly due to high multiplicities in the mid-rapidity region. The response of water Cherenkov detectors and comparisons to other interaction models are shown.

1. Introduction

In this paper, we discuss the high energy limit of hadron nucleus scattering and their influence on air shower properties, as described in Ref. [1]. When approaching highest energies, we expect the differential scattering amplitude to become close to unity. The partons acquire a large transverse momentum of the order of the saturation scale, which leads to an steeper spectrum of forward scattered particles, the most important phase space region for air shower properties.

All air showers in this paper have been computed with the Seneca model [2] using UrQMD 1.3.1 [3] as low-energy model below 100 GeV.

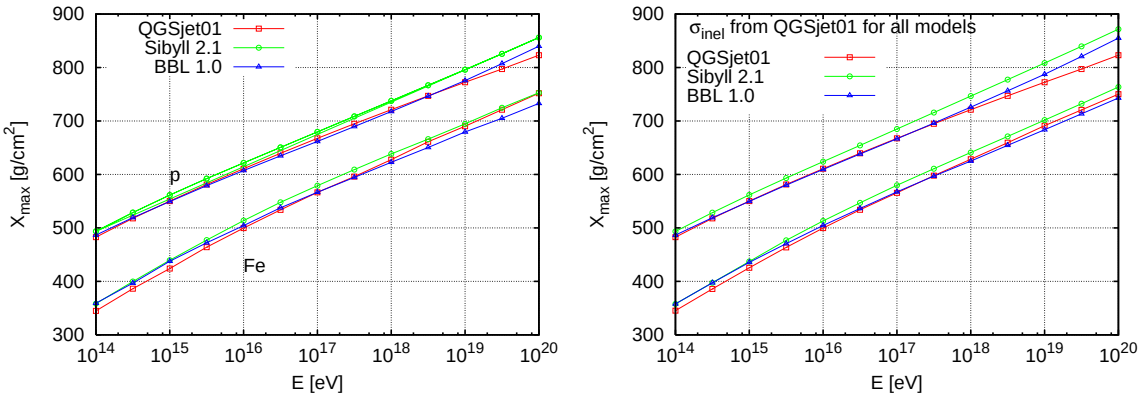

Figure 1. Left panel: $X_{\max}$ as a function of energy. Right panel: $X_{\max}$ of models using inelastic cross-sections from QGSjet01, i.e. differences are due to forward scattering only.

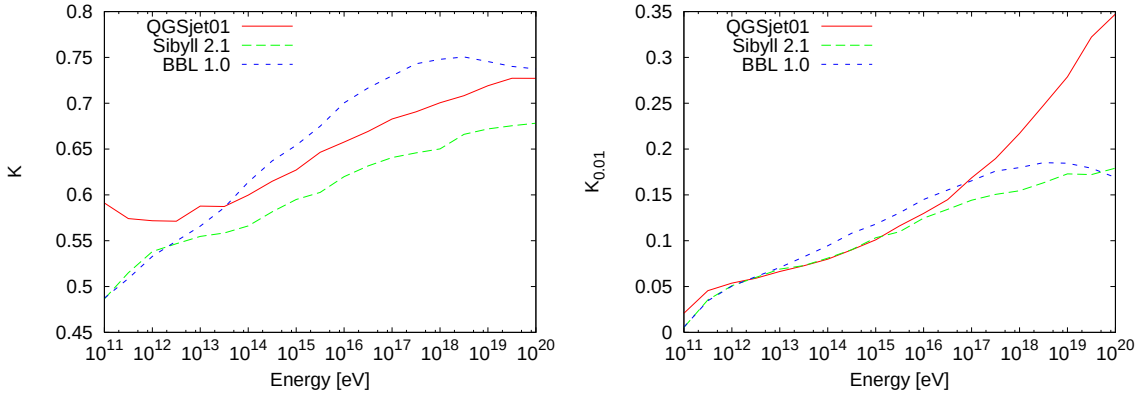

Figure 2. Left panel: Inelasticity of the three models as a function of primary energy. Right panel: Inelasticity $K_{0.01}$, evaluated in the forward phase space region $0.01 \leq x_F \leq 1$.

2. High energy hadron nucleus scattering

When approaching highest energies, higher twist corrections in hadron nucleus collisions become increasingly important. Attempts to account for this are the implementation of an energy-dependent p_t cutoff [4] for hard scattering or the resummation of enhanced pomeron diagrams in an efficient manner [5].

Our approach is to consider the black disk limit (or black body limit - BBL) at high gluon densities within the Color Glass Condensate (CGC) approach[6], where the interaction probability is close to unity. Within this model, the scattering amplitude of a quark on a dense gluon field is resummed to all orders. This can be done since the typical scale of the gluon density, the so-called saturation momentum Q_s is larger than $\Lambda_{\rm QCD}$ and weak coupling methods are applicable.

The Monte Carlo interaction model, which incorporates the physics discussed here has been introduced in Ref.[1] and discussed in more detail in Ref. [7]. The most important feature is the suppression of forward scattering. As a consequence of energy conservation we also find an increase of particle production at lower rapidities. Although less important for the longitudinal profile of an air shower, this results in an increased muon production and is therefore important to be considered when deducing composition from this observable.

Since this approach is only valid when the saturation momentum is large, we use this model only in the high energy/high density limit. For low energies and peripheral interactions we use the standard pQCD Monte Carlo model Sibyll [4].

3. Longitudinal Profile

Results for the mean $X_{\rm max}$ are shown in Fig. 1. The longitudinal profile is dominated by mainly two observables, the forward scattering, often described by the inelasticity ($K = 1 - x_F$ of the fastest particle) and the inelastic cross section which determines the mean free path. Since we have used the inelastic cross sections from Sibyll, differences to this model are due to the reduced forward scattering solely, whereas the difference to QGSjet01 [8] comes from a combination of both different cross sections and inelasticity.

Also shown are the results for iron induced showers computed with the BBL model by simple superposition

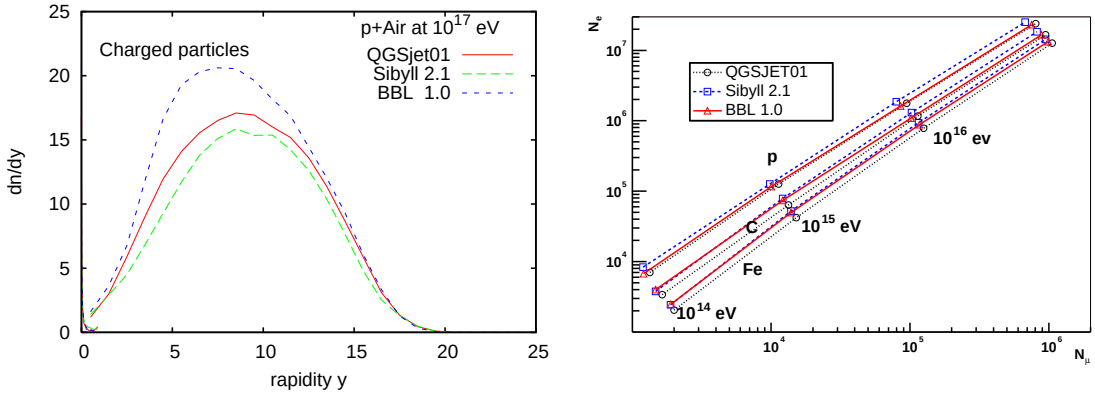

Figure 3. Left: Rapidity of charged particles for p+Air at 10^{17} eV. Right: Electron/positron and muon numbers in the intermediate energy range.

of nucleon-air collisions, just as in Sibyll. This should give a good estimate, since the the running coupling evolution is less sensitive to initial conditions, i.e. the density of the projectile. The full implementation of nucleus-nucleus collisions with consideration of projectile saturation scale will be left for the future.

Fig. 2 shows the inelasticity of the models, defined as mean $1 - x_F$ of the fastest particle. The right panel shows $K_{0.01} = 1 - \int_{0.01}^{1} x_F dn/dx_F dx_F$, which corresponds to the inelasticity averaged over a larger region in forward phase space, not only the fastest particle.

The right panel in Fig. 1 shows $X_{\max}$ for Sibyll and BBL when one applies inelastic cross-sections from QGSjet01 which are somewhat smaller, see e.g. [9]. At largest energies the $X_{\max}$ of Sibyll and BBL get shifted by ca. 15 g/cm^2 and reach 50 and 30 g/cm^2 larger depth than QGSjet, correspondingly. Assuming the same inelastic cross-sections, BBL has a larger $X_{\max}$ than QGSjet01, despite a larger inelasticity of the former. But as can be seen in Fig. 2, QGSjet01 has a larger $K_{0.01}$, as a consequence of a rather flat x-distribution at these energies. Clearly, the inelasticity alone is not sufficient to characterize forward scattering. In Ref. [7] is was shown that $X_{\max}$ is sensitve to the forward region down to $x_F \approx 10^{-2} - 10^{-3}$. Therefore the $K_{0.01}$, or even $K_{0.001}$ variable is more suitable to describe this specific range.

4. Muon- and electron numbers

The major consequence of the implementation of the black body limit is the suppression of forward scattering. However, this also leads to an enhancement of the multiplicity in the mid-rapidity region, see Fig. 3. This has almost no influence on the longitudinal profile, but increases the muon numbers as decay products of low-energy particles. A plot of mean electron/positron and muon numbers is shown in the right panel of Fig. 3. The BBL model seems to interpolate somewhat between the results of Sibyll and QGSjet01, with the transition happening at about 10^{14} eV. Since the primary energy is shared between the nucleons of the projectile nucleus, this interpolation also happens as a function of mass number A at correspondingly higher energy. This can be seen for the carbon projectile in the knee region. Whether this model can help to resolve known problems of models in KASCADE, is subject to a detailed comparison.

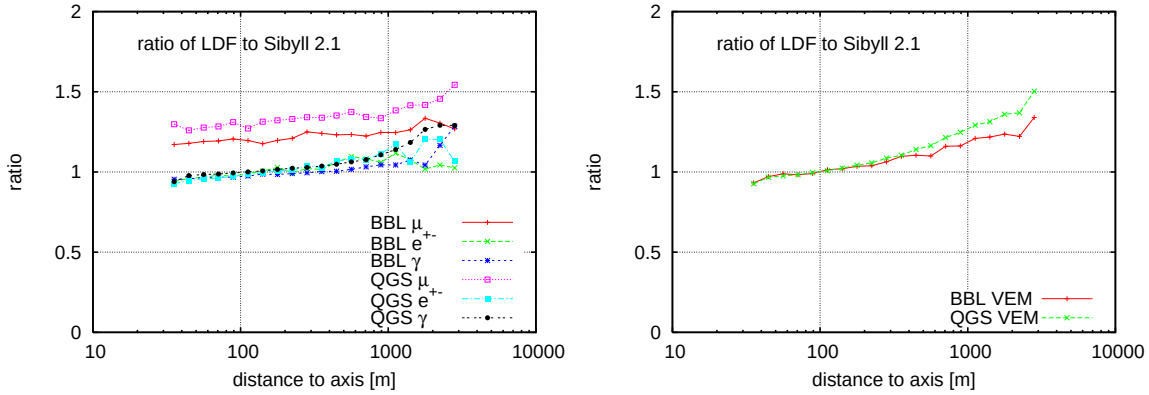

Figure 4. Lateral distribution functions of different particles and of the total signal in VEM units. Results are shown as a ratio to the LDFs from Sibyll. The low energy model ($E < 100$ GeV) is UrQMD.

5. Lateral Distribution Function

In Fig. 4 we show the lateral distribution functions for 10^{19} eV vertical proton showers at Auger altitude. Ratios to the LDFs of Sibyll are plotted. Besides from a small decrease of the slope for electrons and photons, most noticeable is the increased muon number. QGSjet01 shows the same qualitative behavior as BBL. Since muons dominate the VEM signal at large distances, the combined LDF in VEM units shows a significantly flatter slope.

Acknowledgements

The author thanks Adrian Dumitru and Mark Strikman for useful discussions. This work has been supported by BMBF grant DESY 05CT2RFA/7.

References

[1] H. J. Drescher, A. Dumitru and M. Strikman, Phys.Rev.Lett.94:231801,2005
[2] G. Bossard et al., Phys. Rev. D63, 054030 (2001); H. J. Drescher and G. Farrar, Phys. Rev. D67, 116001 (2003).
[3] M. Bleicher et al. *J. Phys.*, G25:1859, 1999; S. A. Bass et al. *Prog. Part. Nucl. Phys.*, 41:225, 1998.
[4] R. S. Fletcher, et al., Phys. Rev. D 50, 5710 (1994); R. Engel, et al., *Prepared for 26th International Cosmic Ray Conference (ICRC 99), Salt Lake City, Utah, 17-25 Aug 1999*.
[5] S. Ostapchenko, proceedings of 13th ISVHECRI, Pylos, Greece, 6-12 Sep 2004, arXiv:hep-ph/0412332.
[6] L. McLerran and R. Venugopalan, Phys. Rev. D 49, 2233 (1994); ibid. 49, 3352 (1994); Y. V. Kovchegov, ibid. 54, 5463 (1996); ibid. 55, 5445 (1997).
[7] H. J. Drescher, A. Dumitru and M. Strikman, proceedings of INFN Eloisatron Project 44th Workshop on QCD at Cosmic Energies: The Highest Energy Cosmic Rays and QCD, Erice, Italy, 29 Aug - 5 Sep 2004, arXiv:hep-ph/0501165.
[8] N. N. Kalmykov, S. S. Ostapchenko and A. I. Pavlov, Nucl. Phys. Proc. Suppl. 52B, 17 (1997).
[9] R. Engel, proceedings of 13th ISVHECRI, Pylos, Greece, 6-12 Sep 2004, arXiv:astro-ph/0504358.